Review

Pyridoxal 5′-Phosphate Biosynthesis by Pyridox-(Am)-Ine 5′-Phosphate Oxidase: Species Specific Features

Maribel Rivero , Nerea Novo , Milagros Medina *

Posted Date: 19 February 2024

doi: 10.20944/preprints202402.1002.v1

Keywords: pyridox-(am)-ine 5'-phosphate oxidase (PNPOx); pyridoxal 5'-phosphate (PLP); flavin mononucleotide; species-specific features; conformational landscape; cofactor channeling

 doi:10.20944/preprints202402.1002.v1

Review

Pyridoxal 5′-Phosphate Biosynthesis by Pyridox-(am)-ine 5'-Phosphate Oxidase: Species Specific Features

Maribel Rivero [1,2], Nerea Novo [1,2] and Milagros Medina [1,2,*]

[1] Departamento de Bioquímica y Biología Molecular y Celular, Facultad de Ciencias, Universidad de Zaragoza, Zaragoza, Spain; miriverob01@gmail.com, nerea.nnh@gmail.com, mmedina@unizar.es
[2] Instituto de Biocomputación y Física de Sistemas Complejos (BIFI), Universidad de Zaragoza, Zaragoza, Spain; miriverob01@gmail.com, nerea.nnh@gmail.com, mmedina@unizar.es
* Correspondence: mmedina@unizar.es

Abstract: Enzymes reliant on pyridoxal 5'-phosphate (PLP), the metabolically active form of vitamin B6, hold significant importance in both biology and medicine. They facilitate various biochemical reactions, particularly in amino acid and neurotransmitter metabolisms. Vitamin B6 is absorbed by organisms in its non-phosphorylated form and phosphorylated within cells by pyridoxal kinase (PLK) and pyridox-(am)-ine 5'-phosphate oxidase (PNPOx). The flavin mononucleotide dependent PNPOx enzyme converts pyridoxine 5'-phosphate and pyridoxamine 5'-phosphate into PLP. PNPOx is vital for both biosynthesis and salvage pathways in organisms producing B6 vitamers. However, for those depending on vitamin B6 as nutrient, PNPOx participates only in the salvage pathway. Transferring PLP produced by PNPOx to client apo-enzymes is indispensable for their catalytic function, proper folding and targeting to specific organelles. PNPOx activity deficiencies due to inborn errors lead to severe neurological pathologies, particularly neonatal epileptic encephalopathy. PNPOx enzymes from different organisms maintain PLP homeostasis through highly regulated mechanisms, including structural alterations throughout the catalytic cycle and allosteric PLP binding influencing substrate transformation at the active site. Despite shared features, species-specific regulations are evident among PNPOx enzymes.

Keywords: pyridox-(am)-ine 5'-phosphate oxidase (PNPOx); pyridoxal 5'-phosphate (PLP); flavin mononucleotide; species-specific features; conformational landscape; cofactor channeling

1. Vitamin B_6: vitamers and metabolism

Vitamins B form a group of 6 hydro-soluble molecules that are essential nutrients in cell bioenergetics and metabolism and that includes thiamine (vitamin B_1), riboflavin (vitamin B_2), niacin (vitamin B_3), pantothenic acid (vitamin B_5), pyridoxine (vitamin B_6), biotin (vitamin B_7), folic acid (vitamin B_9) and cobalamin (vitamin B_{12}). In the case of vitamin B_6, this is the generic name for up to six different vitamers that confer final vitamin B_6 activity: pyridoxine (PN), pyridoxal (PL), and pyridoxamine (PM), as well as their respective 5′-phosphate esters, pyridoxamine-5′-phosphate (PNP), pyridoxal-5′-phosphate (PLP) and pyridoxamine-5′-phosphate (PMP) (**Figure 1A**). Chemically, B_6 vitamers are derivatives of 2-methyl-3-hydroxy-5-hydroxymethyl-pyridine; being their C4 substituent hydroxymethyl ($-CH_2OH$), aminomethyl ($-CH_2NH_2$) and aldehyde ($-CHO$) groups respectively in PN, PM and PL. B_6 vitamers are water-soluble and naturally present in the diet in many forms and foods, added to others, and available as a dietary supplement. Nonetheless, substantial proportions of the naturally occurring PN in fruits, vegetables and grains exist in glycosylated forms that exhibit reduced bioavailability. The biological active form of vitamin B_6 is PLP, functioning as cofactor in nearly 200 PLP-dependent activities carried out by enzymes that account for up to 4% of enzyme-catalyzed reactions [1,2]. Such reactions are included within amino acid and glycogen metabolism, the synthesis of nucleic acids, hemoglobin and sphingomyelin, as well as the biosynthesis and degradation of multiple neurotransmitters [3-5]. PLP is also involved in the

 doi:10.20944/preprints202402.1002.v1

metabolism of one-carbon units, carbohydrates, and lipids, and changes in its physiological concentration contribute to the circadian control of enzyme activities in brain and peripheral tissues [6].

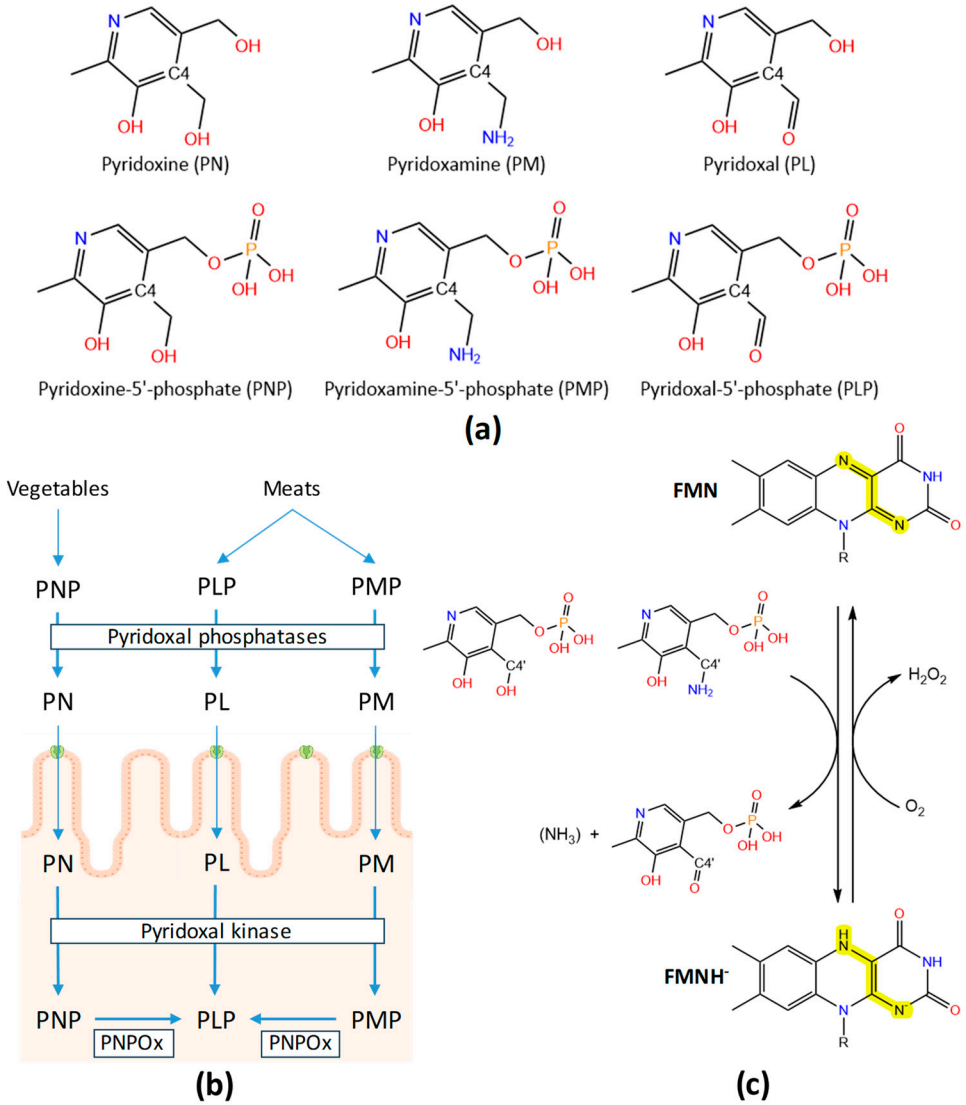

Figure 1. Vitamin B_6. (A) Molecular structures of the B_6 vitamers. **(B)** Overview of PLP metabolism. **(C)** Flavin reductive and oxidative half-reactions during the catalytic cycle of PNPOx.

De-novo pathways for PLP biosynthesis are active only in prokaryotes and plants, in which PNP is, for example, synthesized from deoxy-xylulose 5-phosphate and 4-phosphohydroxy-L-threonine in *Escherichia coli* [7] or from intermediates from the pentose phosphate pathway and glycolysis in other bacteria and plants [8]. In contrast, the salvage pathway is involved in interconversion between different B_6 vitamers, requiring the action of pyridoxal kinase (PLK), pyridox(-am-)ine 5'-phosphate oxidase (PNPOx) and phosphatases, and is active in both prokaryotes and eukaryotes. Therefore, humans must be supplied with this vitamin, being the main sources the diet, degraded PLP-dependent enzymes and the gut microbiota, with the latter making a significant contribution [9]. Dietary deficiency of vitamin B_6 is in general rare, but can occur in the first year of life when the gut flora is not fully established, as well as in patients with chronic alcoholism, diabetes mellitus, coeliac disease, and those on long-term use of isoniazid or penicillamine therapeutic agents [1,10]. The human body only absorbs the non-phosphorylated B_6 vitamers, in a process that occurs in the jejunum portion of the intestine [1,2]. For that, phosphorylated B_6 vitamers are dephosphorylated by

 doi:10.20944/preprints202402.1002.v1

intestinal phosphatases and a glycosidase (**Figure 1B**). The absorption of the pool of non-phosphorylated vitamin B_6 is suggested to occur via passive diffusion across the cell membrane, attached to amino acids/peptides or transported as a sugar adduct, but vitamin B_6 transporters are still to be clearly identified in all type of organisms [9,11,12]. Some studies envisage the existence of PN specific and regulated carried-mediated processes [10,13,14]. Such transport process would be temperature, energy, and pH-dependent, suggesting it may occur by a PN:H^+ symporter mechanism [13,15]. In addition, it also appears to be under the regulation of an intracellular protein kinase A-mediated pathway. More recent studies have also shown that some transporters involved in the uptake of other water-soluble vitamins can also contribute to PN transport, including SLC19A and SLC19A3 [16]. Nonetheless, such possibility of PN transport appears species-specific, and so far no specific transport protein of any mammalian species has been characterized at the molecular level. In *Saccharomyces cerevisiae*, Tpn1p was identified as the plasma membrane vitamin B_6 transporter, with broad substrate specificity for unphosphorylated B_6 vitamers, utilizing a proton symporter mechanism and with residues at its 4-transmembrane segment being key for functionality [17]. Therefore, the roles of different transporters in vitamin B_6 metabolism and their individual contributions to the uptake of PN in different species are areas of ongoing research. PN and PM can be converted to PLP in the intestine cells, prior to transport to the liver or once within it. PM, PN and PL are first re-phosphorylated by PLK, and then, the FMN-dependent PNPOx transforms PMP and PNP into PLP reducing molecular oxygen to hydrogen peroxide (**Figure 1(b)**). Although this occurs mainly in the liver, PNPOx is expressed in all cell types in Eukarya as well as in all type of Bacteria [1]. PLP is exported from the liver bound to albumin; but to enter the brain, it must dissociate and be again dephosphorylated to PL at the blood-brain barrier. Within tissues such as the brain, partial catalysis by PLP or catabolism of PLP enzymes can also lead to production of PMP, which can be converted back to PLP by PNPOx through the salvage pathway.

The versatility of PLP arises from its ability to covalently bind to its client enzymatic substrates, and then to act as an electrophilic catalyst, thereby stabilizing different types of carbanionic reaction intermediates. Within client enzymes, the reactive aldehyde group of PLP generally undergoes a condensation reaction with the amino group of amino acids to produce a Schiff base. In humans, PLP-dependent holoenzymes contain PLP attached by a Schiff base linked to the ε-amino group of a lysine residue at the active site. Moreover, most reactions involve the transfer of PLP to produce a new Schiff base linkage with the amino group of an amino acid at the substrate. B_6 vitamers may also play other roles within the cell, as antioxidants, modifying expression and action of steroid hormone receptors, and on the immune function. PLP has also been reported to exhibit antiepileptic activity, because it is an antagonist of ATP at P2 pyrinoceptor [1]. Nonetheless, PLP is a very reactive molecule and can be very toxic, causing toxicity in the liver and being involved in unwanted reactions [18]. To avoid such processes the cells maintain intracellular levels of free PLP at approximately 1 μM [1]. Several mechanisms contribute to maintaining such low PLP concentrations in cells and body fluids: i) PLP-dependent enzymes that keep it in bound state, ii) inhibition by PLP of PLK and PNPOx, and iii) PLP degradation by phosphatases. In addition, *in vitro* studies suggest that PLP will also be protected intracellularly by being transferred directly from PLK and PNPOx to some of the PLP-dependent enzymes [19].

2. Functional and structural features of human PNPOx

The human *PNPO (HsPNPO)* gene is located in chromosome 17 (17q21.2), encodes for a protein of 261 aa (~30 kDa, Q9NVS9 · PNPO_HUMAN) and has housekeeping characteristics: absence of TATA-like sequences and presence of Sp1-binding sites and, more importantly, CpG islands in the regulatory region. Its mRNA expression is ubiquitous, but its transcription is highly regulated in a tissue-specific manner. Its major sites of expression are liver, skeletal muscle and kidneys, but it is also expressed in the heart, brain and pancreas [20].

 doi:10.20944/preprints202402.1002.v1

Table 1. Summary of kinetic and interaction parameters reported for PNPOx enzymes from different species. .

Species	Conditions	k_{cat}^{PNP} (s^{-1})	K_M^{PNP} (μM)	k_{cat}/K_M^{PNP} (μM^{-1} s^{-1})	k_{cat}^{PMP} (s^{-1})	K_M^{PMP} (μM)	k_{cat}/K_M^{PMP} (μM^{-1} s^{-1})	K_I^{PLP} (μM)	K_I^{PNP} (μM)	K_d^{PLP} (μM)	K_d^{FMN} (nM)	Ref
H. sapiens	50 mM Tris/HCl pH 7.6 37° [1]	0.20±0.01	1.8	0.11	0.20	1.0	0.2	3.2				[21]
	50 mM Tris/BES pH 7.6 37°	0.20±0.01	2.4±0.2	0.08							14±2[2]	[22]
	50 mM Tris/HCl pH 7.6 37°	0.06±0.01	2.6±0.2	0.02				0.6±0.1			13±2	[23]
	50 mM HEPES pH 7.6 37°	0.06±0.01	2.8±0.2	0.02				0.9±0.1				[23]
	50 mM Tris/HCl pH 7.6 37°	0.20±0.01	2.4±0.2	0.08								[24]
E. coli	50 mM Tris pH 7.6 37°	0.3	2	0.15								[25]
	NaPi/HEPES pH 7.6 37°	0.2	2	0.1								[25]
	200 mM Tris-HCl, 200 mM KPi pH 8.5 37°	0.8	2	0.4	1.7	105	0.02	8				[26]
	50 mM Na/HEPES pH 7.6	0.25±0.01	1.6±0.4	0.2				0.28±0.01		0.15		[27]
Sheep brain	100 mM KPi pH 8.0 25°	0.2	13	0.01				4				[28]
	100 mM KPi pH 7.4 25°							2				[29]
Rabbit liver	200 mM Tris pH 8.0 37°		30			10					40	[30]
	200 mMTris/HCl pH 8.0 25°	0.7	8.2	0.1	0.1	3.6	0.03		50	45		[31]
Pig brain	100 mM PPi pH 8.4 25°	0.09	13	0.007	0.009	100	0.00009					[32]

[1] All temperatures are given in Data in ° C. [2] NaPi pH 7.2 25°.

The cDNA for *HsPNPO* was cloned and expressed in *E. coli*, being efficiently overproduced and purified [22]. Once produced, the HsPNPOx protein incorporates FMN as cofactor, which enables it to catalyze the conversion of both PNP and PMP to the biologically active PLP (**Figure 1(b)**). Thus, HsPNPOx is able to oxidize both a primary alcohol and a primary amino to an aldehyde being equally efficient with both substrates [25]. Catalysis occurs by the initial transfer of a pair of electrons (as a hydride) from the C4' of PNP (or PMP) to the tightly bound FMN, forming $FMNH^-$ and PLP, during the so-called flavin semi-reductive half-reaction (**Figure 1(c)**). Then, the electron pair is transferred in the oxidative half-reaction to O_2, regenerating oxidized FMN and forming H_2O_2 (di Salvo et al., 2002). HsPNPO was confirmed to be a homodimer that presents characteristic absorption maxima for a flavoprotein at 276 nm, 385 nm and 448 nm [21]. Noticeably, HsPNPOx exhibits considerably low k_{cat} as well as K_M for both PNP and PMP, with affinities for both substrates being in the low micromolar range (**Table 1**) [21]. Steady-state studies revealed a pre-steady state transient period where rate of PLP synthesis was slower than normal, and thought to be consistent with the few seconds whilst enzyme and substrate form the complex. Despite FMN of HsPNPOx masked spectroscopic observation of tightly bound PLP, the strong binding of PLP to apo-HsPNPOx was spectroscopically confirmed (peak at ~410 nm). Thus, PLP was reported as an effective product/competitive inhibitor of HsPNPOx. However, the catalytic activity of preformed HsPNPOx:PLP complexes did not appear

 doi:10.20944/preprints202402.1002.v1

to be affected *in vivo*, because K_i^{PLP} is not low enough for it to be tightly bound at the active site. This indicated that tight binding of PLP occurs at an alternative non-catalytic site, and suggested that a tunnel may exist between the active site and the secondary non-catalytic site [33]. This allosteric PLP binding site is key in enzyme regulation, produces allosteric inhibition and has been proposed to act protecting PLP from nucleophiles as well as in its channelling to client apo-enzymes. Nonetheless, in HsPNPOx coupling between catalytic and allosteric sites appears to be weak, allowing formation of complexes with PLP at the allosteric site and PNP at the catalytic site that still remain partially active [23]. Moreover, while free HsPNPOx shows its active site open, formation of the HsPNPOx:PLP complex partially closes it because of the bound PLP blocking solvent access.

The PDB contains five structures for HsPNPOx; two of the wild-type (WT, PDB ID 1NRG and 8QYT) and three corresponding to the mutants, R229W (3HY8), R116Q (6H00) and R225H (8QYW) [21,22,34]. The structures for the WT and R229W variants are complexes with PLP, showing it in close proximity to the FMN cofactor at the active site. On their side, the structures of the R116Q and R225H variants correspond to the PLP free protein. In general, they do not show the first 48-50 N-terminal residues because of their high predicted disorder. The functional HsPNPOx structure is a homodimer with a FMN and a substrate binding site in each monomer (**Figure 2(a)-(b)**). Each HsPNPOx monomer exhibits a two-domain architecture represented by two PFAM domains [21]. The larger domain, a Putative_PNPOx domain (PFAM: PF01243, IPRO11576, residues 75-153), is formed by 6 β-strands and 2 short α-helix, while the smaller domain, a PNP_phzG_C domain, is made up of 5 β-strands (PFAM: PF10590.9, IPRO19576, 206-261). In addition, 1 additional α-helix precedes the Putative_PNPOx domain, and 3 more make the inter-domain link (residues 154-205) between PFAM domains (**Figure 2(b) and 3**). Several of the β-strands organize in β-hairpins and all of the make a β-sheet. The functional dimer is stabilized by salt-bridge interactions between the two monomers, particularly Arg116-Glu143 and Arg181-Asp228. The enzyme contains up to six Cys residues by monomer that apparently are not involved in catalytic activity, although two of them, Cys82 and Cys86, might be implicated in Cys82-Cys82 and Cys86-Cys86 disulphide bonds formed at the interface between both monomers (**Figure 2(b)-(c)**). FMN locates in a deep cleft formed by the two protein domains, interacting with both monomers (both by H-bond and water-mediated links) and contributing to inter-subunit interactions (**Figure 2(a)-(c)**). These interactions stabilize FMN binding and may also ensure the correct isoalloxazine orientation for the catalytic activity. Residues participating in these interactions are Thr111, Gln139, Arg141, Gln174, Ser175, Glu217, Trp219 and Arg229, with the later making an ion-pair with the phosphate of FMN (**Figure 2(c)**) [21]. Additionally, both protein domains and monomers are involved in PLP binding at the active site. The WT HsPNPOx:PLP structure shows the C4′ of PLP situated in front of N5 at the *re* face of FMN, with the phosphate group pointing out of the cavity mouth and interacting with residues from both monomers: Lys100A, Tyr157A, Arg161A, Ser165A and Arg225B (**Figure 2(c)**). The pyridine ring stacks against the isoalloxazine of FMN and is allocated within residues of both chains in the homodimer: Glu77A, Trp206A, Arg225B and His227B. In particular, Arg225 and His227 orientate substrate binding for catalysis, placing the substrate pyridine ring parallel to the FMN isoalloxazine ring, so the distance between the C4′ of PNP and the N5 of FMN would allow efficient hydride transfer [22]. With the only exception of Glu77, these residues are highly conserved in other species (**Figures 3 and 4**).

 doi:10.20944/preprints202402.1002.v1

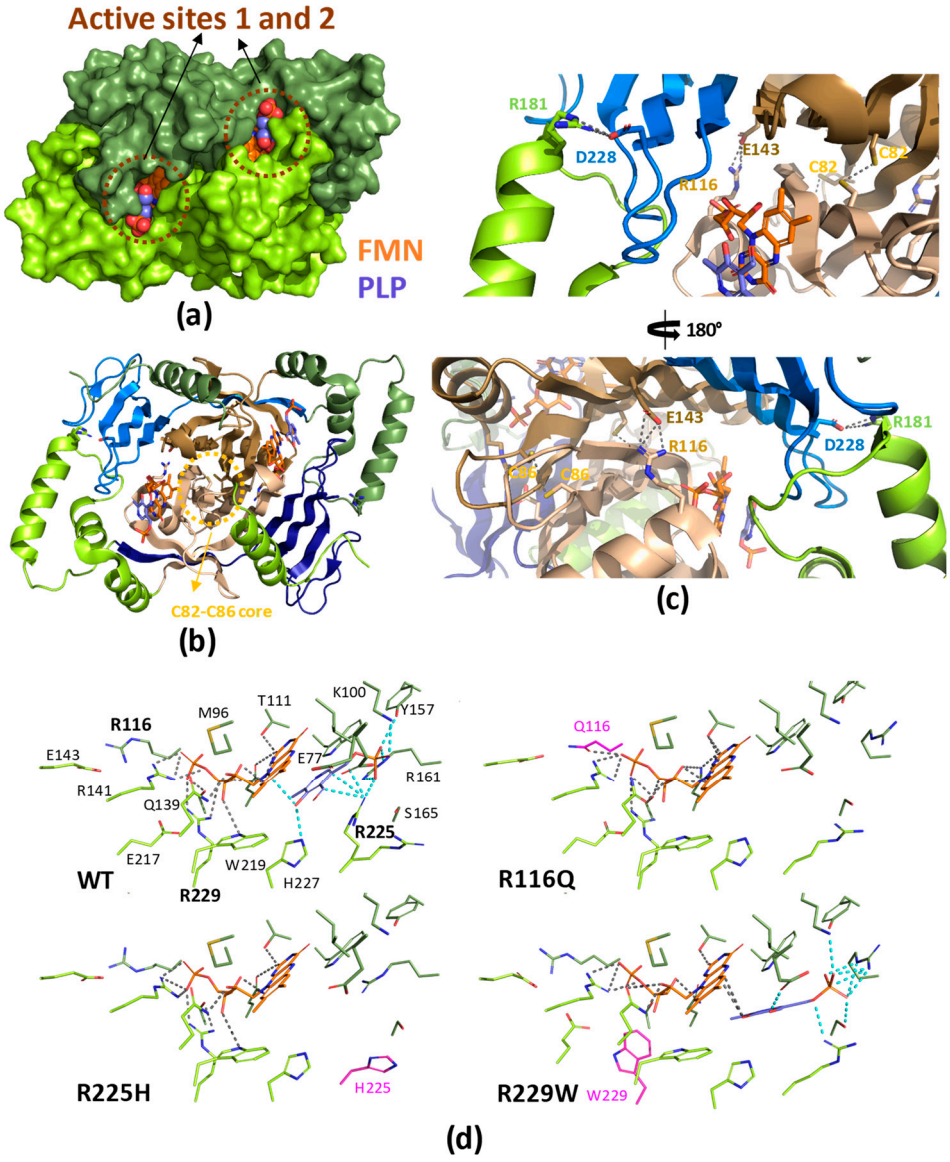

Figure 2. Structural features of HsPNPOx. (a) Surface representation of the crystallographic structure of WT HsPNPOx homodimer in complex with PLP at the active site (PDB 1NRG). **(b)** Cartoon model of the homodimer, with the Putative_PNPOx domains in each protomer highlighted respectively in dark and light sand and the corresponding PNP_phzG_C domains in light and dark blue. Residues involved in potential inter-subunit contacts are highlighted in sticks. **(c)** Detail of inter-subunit contacts. Top and bottom panels correspond to the view centred at the FMN of one active site upon 180° rotation. **(d)** Detail of the active site environment in the WT in complex with PLP, the R116Q mutant (6H00), the R225H mutant (8QYW) and the R229W mutant in complex with PLP (3HY8). Mutated residues are highlighted in magenta. Polar contacts for FMN and PLP are shown as dashed lines in grey and cyan respectively. Other colour codes as in panel (a). In all panels, one protomer of the homodimer is shown in smudge green and the other in lemon green, while FMN and PLP are respectively shown in CPK coloured orange and violet spheres or sticks. Figure produced using PyMOL [35].

Preprints.org (www.preprints.org) | NOT PEER-REVIEWED | Posted: 19 February 2024 doi:10.20944/preprints202402.1002.v1

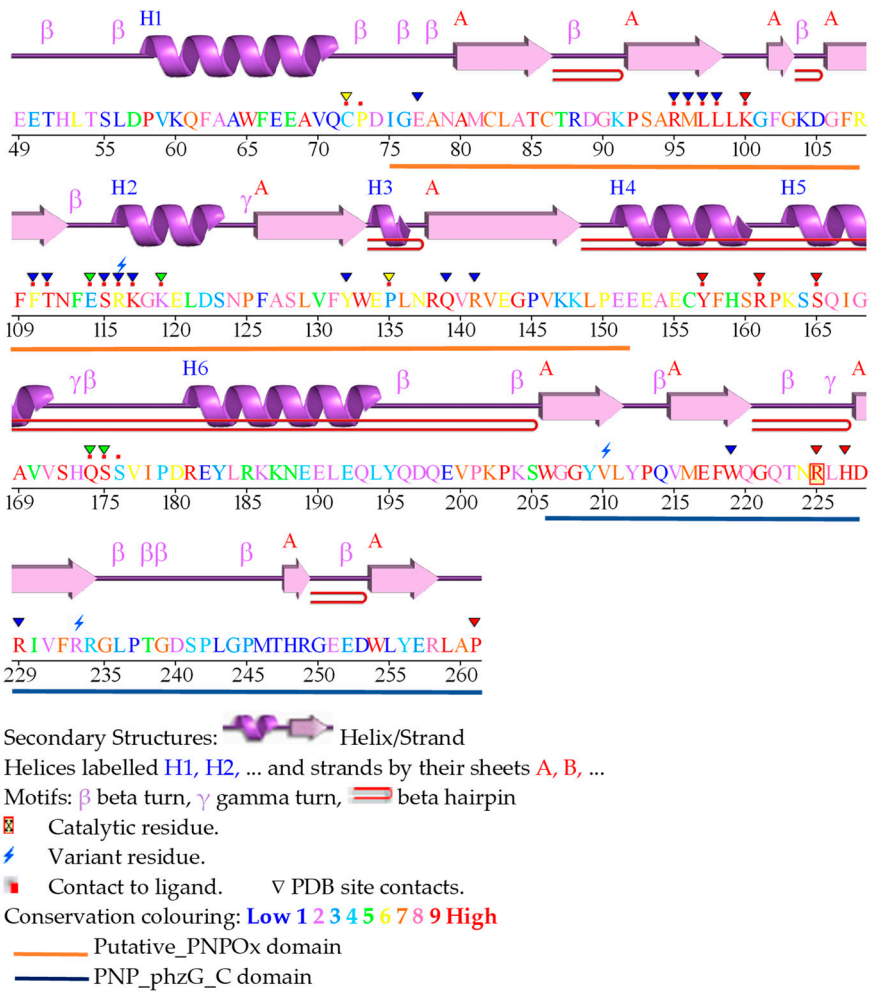

Figure 3. PDBsum analysis of HsPNPOx. Secondary structure analysis as obtained by PDBsum server (https://www.ebi.ac.uk/thornton-srv/databases/pdbsum/) for PDB 1NRG.

As above indicated, the R225H PNPOx variant is one of the few for which the crystal structure is available (PDB 8QYW). The mutation hardly has any impact in the overall fold (RMSD ~0.3 Å) and active site architecture of the protein, but this replacement will prevent the correct coordination of the phosphate of PLP and the correct allocation of the substrate for catalysis (**Figure 2(d)**). The replacement of Arg229 with a Trp is also among the best biochemically characterized mutations of HsPNPOx (PDB 3HY8). R229W mutant and WT structures show identical overall folds (RMSD ~0.6 Å), but the mutation leads to the loss of the interaction of residue 229 with the phosphate of FMN as well as to a change in the electrostatics for FMN binding. Substituted W229 is too big to be accommodated at the FMN binding pocket, inducing a movement in the loop containing His227 and Arg225 to relieve steric interaction and producing as result the loss of two other critical H-bonds (**Figure 2(d)**). Structural perturbation of the R229W mutation affects not only the FMN phosphate binding site but also the substrate binding site, because it removes critical H-bond interactions of the substrate with His227 and Arg225. Therefore, substrate binding orientation is apparently altered, being the PLP and FMN ring moieties no longer parallel (**Figure 2(d)**). As will be discussed below, this mutation impacts the affinities of FMN and PNP, as well as hydride transfer efficiency [22]. The other pathogenic variant for which a crystal structure is available is R116Q. Arg116 is located at the N-terminal end of the α-helix whose positive dipole charge might stabilize the negative charge of the FMN phosphate. In addition, it also makes an ion-pair interaction with the neighboring Glu143 residue from the other protomer **(Figure 2(d))**. No major differences are found in the R116Q mutant overall structure when compared to the native protein. However, the Gln side chain being shorter than that of the Arg leaves the introduced amide at bonding distance of the FMN phosphate but not

 doi:10.20944/preprints202402.1002.v1

of Glu143. Therefore, in solution, this replacement might have a direct impact on FMN affinity as well as on homodimer stability and/or inter-subunit flexibility.

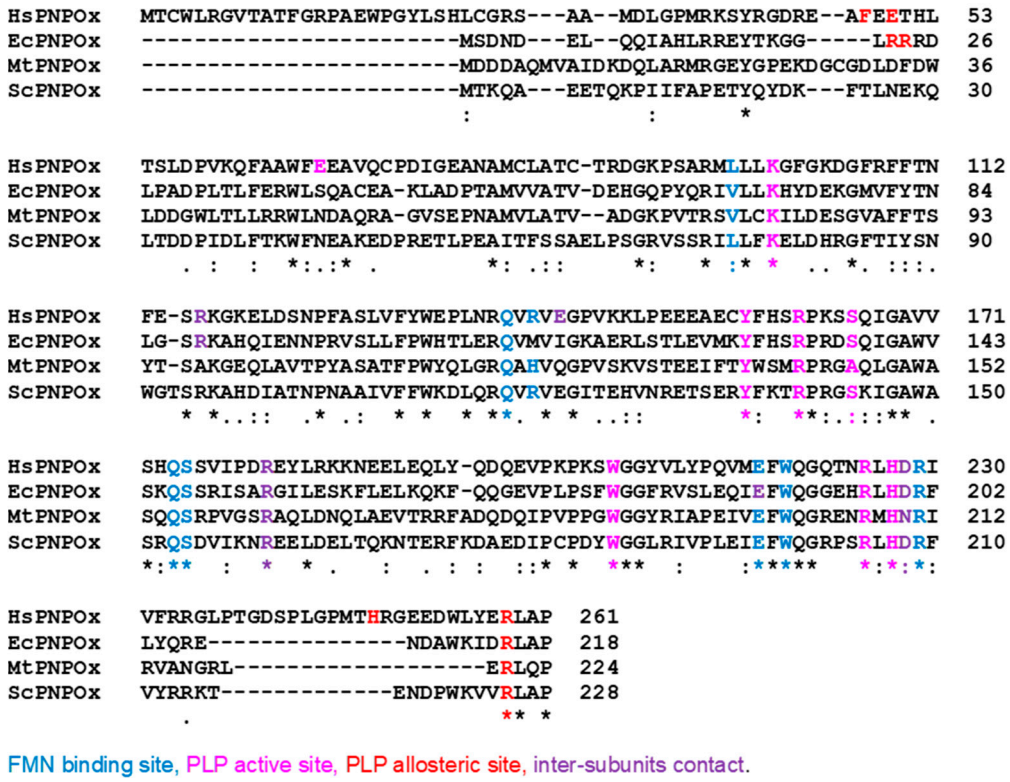

Figure 4. Multiple sequence alignment (MSA) (Clustal Omega) of WT PNPOx sequences from species with available crystallographic structures. Asterisk (*), colon (:) and period (.) symbols indicate respectively identical residues, conserved substitutions and semi-conserved substitutions. Colours highlight residues involved in binding of particular ligands or inter-subunit binding.

3. The human PNPOx enzyme in disease

Binding of the PLP product of HsPNPOx to its client apo-enzymes is essential for their catalytic function, and in many cases also for their correct folding and targeting to the right organelle [19]. Moreover, considering the large number of reactions relying on PLP, including particularly its vital role in neurotransmitter metabolism (synthesis of inhibitory transmitter GABA), severe neurological disorders, such as convulsions and epileptic encephalopathy, result from a reduced availability of PLP in the cell [36,37]. Such deficiency is in many cases due to inborn errors in the enzymes of the salvage pathway. In particular, in patients suffering of PNPOx deficiency (PNPOD, OMIM #610090), PLP cannot be synthesised from dietary PN (present in vegetables and added as a B_6 supplement to infant formulae and parenteral nutrition), nor can it be regenerated by recycling of PMP. Due to its key role in brain metabolism, the mutation or deficiency of this enzyme in humans is linked to neurological pathologies, being neonatal epileptic encephalopathy the most remarkable one [38,39]. PNPOD is an autosomal recessive inborn error of metabolism that leads to seizure disorder, presenting in the new-born period or early infancy [40]. Clinical phenotypes and other general features observed include foetus distress, hypoglycaemia, acidosis, anaemia and asphyxia [22]. Progressive deterioration can lead to death within weeks. Cerebrospinal fluid and urine analyses indicate reduced activities of PLP-dependent enzymes in PNPOD. Under such situations, surviving children are usually mentally retarded and have dependence on vitamin B_6 in the form of PLP [22]. Moreover, genome-wide association studies identified an important susceptibility locus for genetic generalized epilepsies at 17q21.32 (rs72823592), the closest gene to which is *HsPNPO*, suggesting that mild PNPOx deficiency could be a susceptibility factor for genetic generalized epilepsies presenting

 doi:10.20944/preprints202402.1002.v1

at various ages [40]. PNPOD is a potentially treatable disease that for many years has been under or misdiagnosed due to the lack of specific biomarkers [41-43]. Treatment with PLP has been shown to be very effective in controlling seizures in PNPOD, with some patients even showing normal development and the treatment being lifelong [44]. On the contrary, with late or no treatment, patients die or show severe mental handicap. Some PNPOD seizures were observed to respond to treatment with PLP but not to PN [40], nonetheless some patients' seizures responded also to PN treatment [45] and others responded to PN but not to PLP [42]. Different susceptibility of patients to PLP or PN treatments, as well as individuals showing from severe to mild phenotypes, are explained because PNPOD can be caused by different point and non-sense mutations as well as deletions/insertions and frame shifts in the *HsPNPO* gene (see Table 3 in [38]). For these reasons, treatment of PNPOD has been relatively complicated. Some mutations (such as R225H) have in fact been reported to be responsive to PN but not to PLP, which seemed to inhibit the mutant's activity instead. Others (R225H/C and D33V), result in seizures more likely to be responsive to PN, while some (R116Q) dramatically affect erythrocyte PNPOx activity. In general, mutations affecting PLP binding can be treated with PN (but worsen after treatment with PLP), while mutations affecting FMN binding can only be treated with PLP. In addition, the riboflavin status, which might work as a pharmacological chaperon in selected PNPOx variants failing FMN binding, or the adequate supply of vitamin B_6 to the foetus by the mother have been pointed as factors positively influencing treatment response [1,40].

Naturally occurring HsPNPOx variants have been separated in categories based on their position in the protein structure and type of mutation (see Figure 3 and Table 3 in [38]). The most populated category contains mutations that directly affect the catalytic site and impair coordination by positively charged residues of phosphates of PLP and FMN at their binding sites (namely R95C, R116Q, R141C, R161C, R225C/L/H, and R229W/Q). Some of these mutations can also produce loss of PLP π-stacking interactions (mutations at Arg225) or inter-chain bonds (R116Q). The next category groups mutations affecting protein fold and stability due to non-conservative substitution, with impacts ranging from mild loss of stabilizing surface (E50K) and hydrophobic (P213S) interactions to destabilizing clashes (G118Q/R). Another category groups variants with a loss of residues (deletions, stop codons, frame shifts, non-sense mutations, etc), disrupting the compact structure of the PNPOx homdimer and consequently the production of a functional protein. The last group includes a N-terminal extension that might mildly affect its potential unknown function.

Pathogenic mutations for which structural information is available, namely at Arg225, Arg229 and Arg116 in HsPNPOx, have also been biochemically studied. The R229W missense mutation was soon related to neonatal epileptic encephalopathy as a consequence of drastic decrease in PNP oxidase activity and failure in maintaining PLP levels, while the R229Q mutation produced moderate global developmental delay [22,46]. Seizures produced by the R229W mutation were resistant to PN but ceased after PLP treatment, and similarly patients suffering from the R229Q mutation reduced seizures when treated with PLP [40,45]. R229W and R229Q mutations affect the last arginine in a highly conserved sequence –RLHDR- that contributes to bind FMN tightly to the active site (**Figure 4**). *In vitro* studies indicated that the R229W and R229Q mutations have no impact on overall structural integrity, including homodimer formation and conformational thermal stability. Nonetheless, their k_{cat} values resulted 4.5- and 3.6-fold lower than those of WT, while K_M^{PNP} increased by 192- and 129-fold respectively [22]. In addition, both mutants showed a decrease in FMN affinity (K_d^{FMN} respectively being 50-fold and 3-fold higher than WT). Therefore, both pathogenic mutants, but particularly R229W, lead to a significant decrease in catalytic efficiency (k_{cat}/K_M). As above indicated, the crystal structure of the R229W variant shows structural alterations in the active site (**Figure 2(d)**): loss of H-bond and salt-bridge interactions of FMN with Ser175 and Arg229, as well as loss of critical H-bonds involving His227 and Arg225, important residues for substrate binding and orientation for catalysis. Unlike Trp, Gln has a similar size to Arg, suggesting that in this case steric interference may not be a factor for observable changes in oxidase activity. Loss of H-bonds between Ser175 and Glu217 with FMN could explain reduced affinity. While R229W lost FMN quite easily during purification, remaining residues in the FMN binding pocket ensured its binding and catalytic

 doi:10.20944/preprints202402.1002.v1

orientation. Most likely Gln229 in R229Q can still H-bond with FMN and does not alter significantly other interactions in the pocket.

In agreement with the above indicated structural information, the conformational characterization of R116Q HsPNPOx suggested that the mutation does not alter overall structure integrity, despite affecting the enzyme's thermal stability. This observation agrees with the mutation preventing one of the salt bridges that stabilizes the interface between both protomers in the homodimer. This has an impact on the enzyme affinity for FMN (K_d^{FMN} 20-fold higher than WT), which sits at the interface between protomers, and as a consequence on the catalytic efficiency that is reduced up to 40% of that of WT due to a decrease in k_{cat} and increase in K_m^{PNP}. The R116Q mutation has been shown to hardly reduce PLP affinity, but it impairs the transfer of PLP to PLP-dependent enzymes, reducing the reactivation of the corresponding apo-enzymes [47,48]. Such impairments have also been observed in other mutations, such as R95C, and might have drastic effects on neurotransmitters biosynthesis.

Other HsPNPOx pathogenic variants responsible for PNPOD have also been more recently evaluated, namely G118R, R141C, R225H, R116Q/R225H, and X262Q (replacement of the stop codon with a glutamine residue, leading to the formation of a 28-amino-acids-longer protein at the C-terminal end) [23]. As the above described mutations, these replacements also mainly negatively impact substrate and FMN cofactor binding and, as a consequence, the enzyme catalytic activity, but in general, they hardly impact the enzyme allosteric properties.

4. Functional and structural features of *Escherichia coli* PNPOx further contributed to understand enzyme regulation

The *E. coli* PNPOx (EcPNPOx) is one of the best studied. In addition to participating in the PLP salvage pathway, as HsPNPOx, it is also the last enzyme in the *de-novo* PLP biosynthesis pathway, being key in PLP homeostasis and bioavailability [18]. Differently to HsPNPOx, EcPNPOx greatly favors transformation of PNP over PMP (K_m^{PMP} 50-fold higher than K_m^{PNP}) [26]. Nonetheless, and despite its relevant function, EcPNPOx is also a poorly efficient enzyme (**Table 1**). EcPNPOx was soon shown to be controlled by inhibition of its PLP product, as well as to bind PLP tightly at a secondary non-catalytic site on each monomer, remaining bound during size-exclusion chromatography and purification but readily able to be transferred to PLP-client enzymes [49]. Thus, the EcPNPOx non-catalytic site was proposed to sequester PLP to channel it to client enzymes. More recently, mutagenesis, kinetic and equilibrium studies have demonstrated that PLP inhibition of EcPNPOx is actually of a mixed-type resulting from product binding at the allosteric non-catalytic site, pointing also to structural and functional connections between the active and the allosteric sites [27]. Thus, EcPNPOx would suffer an allosteric feedback inhibition where binding of substrate at the active site and binding of PLP at the allosteric site negatively affect each other. This would produce a non-competent catalytic PNP-EcPNPOx–PLP ternary complex that reduces the ability of PLP to bind at the active site. Moreover, since binding of PLP at the non-catalytic allosteric site of free EcPNPOx has higher affinity than binding at the active site, PLP will preferentially bind to the allosteric site in the free enzyme.

Several crystallographic structures are reported for EcPNPOx (**Figure 5**). This includes structures of WT both free (1WV4, 1DNL) and in complex with PLP at the active site as well as at other different sites (1G76, 1G77, 1G78, 1G79, 1JNW). Recently, structures of a mutant (K72I:Y129F:R133L:H199A) whose active site is impaired have been reported both free and in complex with PLP at the non-catalytic allosteric site (respectively 6YLZ and 6YMH). Despite some structural variations, the overall folding and binding sites for the FMN and the catalytic substrate are highly conserved in comparison to HsPNPOx (**Figure 5(a)-(b)**). Hydrophobic interactions of FMN isoalloxazine with Val69A and Trp191B (Leu97A and Trp219B in HsPNPOx) are conserved. FMN also contributes to inter-subunit interactions, both direct and water-mediated, that are mostly conserved across species (**Figure 5(c)**). Main differences relate to Arg88 and Met113 (Arg116 and Arg141 respectively in HsPNPOx). In EcPNPOx, Arg88 bridges both the phosphate moiety of FMN and the side chain of Glu189, while in HsPNPOx the corresponding Arg116 participates in an inter-

 doi:10.20944/preprints202402.1002.v1

subunit salt-bridge with Glu143 (Ile115 in EcPNPOx). On its side, Met113 in EcPNPOx does not support the stabilization of the phosphate group of FMN, contrary to the anchoring provided by Arg141 in HsPNPOx. In addition, the Arg153-Asp200 inter-subunit interaction appears more sluggish in the EcPNPOx structures than the corresponding Arg181-Asp228 one in HsPNPOx. Nonetheless, all residues at the PLP catalytic site remain strictly conserved in EcPNPOx compared to its human homologue (**Figure 5(d)**).

The available EcPNPOx crystal structures show different unit cells and active site conformations that range from open conformations in the absence of PLP, to partially or closed conformations in their presence, as well as through conformations showing major disorder [50]. In general, PLP binding causes residues 129-140 and 193-199 to move towards the active site, allowing Tyr129, Arg133, Ser137, Arg197 and His199 to interact with PLP, making the active site partially but not completely closed (**Figure 5(d)**). The N-terminus appears quite flexible in general and is predicted as disordered, but some structures show that it might fold in an α-helix that stretches over the mouth of the active site to sequester bound PLP, with Arg14 and Tyr17 H-bonding it [18,50] (**Figure 5(e)**). Comparison of such crystal forms with data from mutational analyses allowed to envisage a molecular mechanistic pathway for EcPNPOx [50]. It will initiate with the binding of PNP at the active site of the resting enzyme. Subsequently, the catalytic stage will produce PLP, and finally the PLP product will be transferred from the active site to the allosteric site for subsequent transfer to vitamin B_6 apo-enzymes [33]. These studies also showed a relevant role for Arg197 (**Figure 5(d)**), both in binding and catalysis, with its guanidinium side chain being key in determining the enzyme stereospecificity, and contributing to accept the pair of electrons on C4' of PNP that are transferred to FMN as a hydride ion [50].

 doi:10.20944/preprints202402.1002.v1

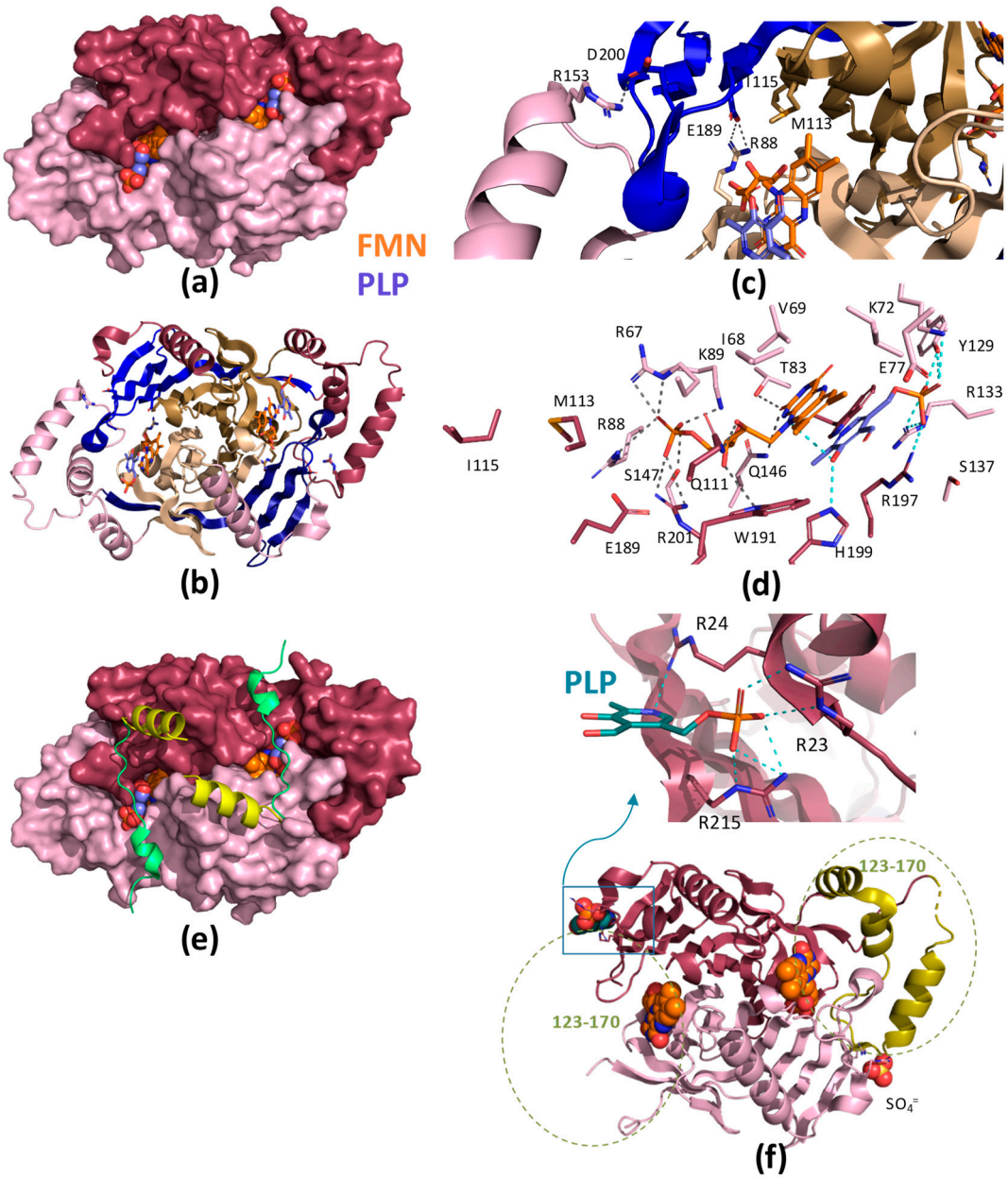

Figure 5. Structural features of EcPNPOx. (a) Surface representation of the crystallographic structure of WT EcPNPOx homodimer in complex with PLP at the active site (PDB 1G77). **(b)** Cartoon model of the homodimer, with the Putative_PNPOx domains in each protomer highlighted respectively in dark and light sand and the corresponding PNP_phzG_C domains in light and dark blue. Residues involved in potential inter-subunit contacts are highlighted in sticks. **(c)** Detail of inter-subunit contacts at the FMN of one active site. **(d)** Detail of the active site environment in the WT structure in complex with PLP. Polar contacts for FMN and PLP are shown as dashed lines in grey and cyan respectively. Other colour codes as in panel (a). **(e)** N-terminal tail as observed in some structures in the active site environment. Position of the N-terminal is shown as cartoon at each protomer in a PNPOx free structure (PDB 6YLZ, yellow tail) and in a complex of PNPOx with PLP (PDB 1JNW, light green), while the rest of the structure is shown as surface. **(f)** Structure of a quadruple mutant at the active site of EcPNPOx with a PLP molecule bound at one of the allosteric sites and a sulphate ion at the other (PDB 1YMH). The inter-domain region observed only in one of the protomers is highlighted in pale green, and its position in both protomers is highlighted by a dashed circle of the same colour. In all panels, one protomer of the homodimer is shown in raspberry and the other in pale pink. FMN, PLP at the active site and PLP at the allosteric site are respectively shown in CPK coloured orange, violet or green teal spheres or sticks. Figure produced using PyMOL [35].

 doi:10.20944/preprints202402.1002.v1

Mutagenesis and structural analysis have situated the allosteric PLP binding site in EcPNPOx at the interface between protomers and formed by an intricate electrostatic arginine cage comprised of Arg23, Arg24, and Arg215 (the three within the same protomer) that effectively captures PLP through its phosphate group (**Figure 5(f)**) [18]. Manipulation of EcPNPOx allosteric properties has been achieved through site-directed mutagenesis targeting the arginine cage, unveiling a spectrum of effects ranging from the relaxation of allosteric coupling (observed in R23L/R24L and R23L/R215L variants) to the complete abolition of allosteric properties (as seen in R23L/R24L/R21L). Noticeably, the crystal structure of this EcPNPOx-PLP-non-catalytic complex exhibits large structural asymmetry. Specifically, only the allosteric arginine cage in one monomer tightly binds PLP, while helices 123-130, 135-143, and 153-166 in the other monomer (forming the interdomain cap that folds out of the PNPOx and PNP_phzG_C domains) undergo disorder upon PLP binding (**Figure 5(f)**). Such disorder is particularly localized to the surface cleft between the arginine cage of the first monomer and the N-terminal portion of helix 153-166 in the other monomer.

Altogether, these observations offered valuable insights into the allosteric regulation of EcPNPOx activity [18]. Thus, researchers in the field have shown that EcPNPOx is regulated by an allosteric inhibition mechanism that makes the EcPNPOx-PNP-PLP ternary complex catalytically incompetent. Such regulation occurs between two binding events, PNP and PLP, as a consequence of the structural perturbations induced on the protein by both upon binding. PLP binding at the Arg cage produces an important rearrangement at the active site, displacing some highly conserved residues regarding both the FMN and the PNP substrate, and thus preventing the correct orientation of the substrate for stereospecific hydride transfer to FMN. Similarly, PNP binding at the active site is expected to impact PLP binding at the allosteric site, aligning with studies envisaging flexibility at the monomer inter-domain region contributing to widen the channel for PLP passage between active and allosteric sites [33,40]. In this way, the enzyme's function might be finely tuned through structural perturbations induced by the binding of both PNP and PLP. In addition, tight binding of PLP to the allosteric site in EcPNPOx will protect against the reactivity of its aldehyde group from the environment, while allowing its concerted transfer to PLP-dependent apo-enzymes. Hence, implying the involvement of EcPNPOx in facilitating the intracellular PLP delivery process.

5. PNPOx species-specific features

In addition to HsPNPOx and EcPNPOx, early studies reported kinetic and interaction parameters for PNPOx from various mammalian sources (**Table 1**), showing that, in general, PNPOx binds FMN with affinities in the nM range and is, at least *in vitro*, a relatively inefficient enzyme from a catalytic standpoint. Thus, PNPOx enzymes are characterized by sluggish k_{cat} values, with K_m and K_d values for substrates and the PLP product generally falling in the low micromolar range. Crystallographic structures are also available for PNPOx from the yeast *S. cerevisiae* (ScPNPOx, PDB 1CI0) and *Mycobacterium tuberculosis* (MtPNPOx, PDB 2A2J), but none of them has been functionally evaluated (**Figure 6**). Sequence identity within the assessed mammalian PNPOx states exceeds 90% (**Table 2**), but it decreases to around 40% when comparing mammalian enzymes to any of the others (**Table 2**). Moreover, pairwise sequence identity among ScPNPOx, EcPNPOx and MtPNPOx also ranges 40%, envisaging distinctive features among them.

Table 2. Percentage of sequence identity among PNPOx enzymes from different species structurally or functionally characterized.

Species	HsPNPOx	EcPNPOx	MtPNPOx	ScPNPOx	Rabbit	Pig	Sheep
HsPNPOx	100						
EcPNPOx	43.8	100					
MtPNPOx	38.1	41.5	100				
ScPNPOx	38.1	41.6	37.8	100			
Rabbit	91.2	40.5	38.4	39.7	100		
Pig	89.7	41.5	38.0	38.0	87.0	100	

 doi:10.20944/preprints202402.1002.v1

Sheep	89.7	43.0	42.5	41.2	87.0	88.9	100

Particularly worth to note are those at the N-terminus, where HsPNPOx is approximately 25 residues longer than EcPNPOx, MtPNPOx, and ScPNPOx. Moreover, in HsPNPOx the first 46-48 residues are predicted as disordered and only a few of them are seen in some of the reported structures. A similar scenario occurs in general for the 19-25 N-terminal residues in the shorter homologues. In fact, this N-terminus hardly exhibits conservation among species (**Figures 3 and 4**), with Tyr41 (number corresponding to HsPNPOx) being the only apparent conserved residue. This Tyr41 together with Asp44 replace Arg14 and Tyr17 in EcPNPOx, which have been proposed to block the access to the active site during the catalytic cycle (**Figure 5(e)**). Noticeably, in HsPNPOx they were proposed as candidates to also H-bond to PLP creating a lid over the active site as the other residues would do in EcPNPOx [21]. Asp44 is also conserved in ScPNPOx and shows a conservative replacement in MtPNPOx. Additionally, EcPNPOx includes in this N-terminal region a part of the key motif (Arg23-Arg24) implicated in the PLP allosteric site that is absent at the N-terminus of the other evaluated enzymes. Interestingly, another significant insertion (15-20 residues) near the C-terminus of HsPNPOx (**Figure 4**) results in a considerably longer loop compared to ScPNPOx, EcPNPOx and particularly MtPNPOx (where it is almost non-existent) (**Figure 6**). This makes the structure of HsPNPOx unique at the loop connecting the C-terminal β-hairpin This observation may be solely structural without a direct catalytic role, but the terminal β strand contains a highly conserved Arg, Arg258 in HsPNPOx, that corresponds to the third Arg cage residue (Arg215) identified in the PLP allosteric site in EcPNPOx. Noticeably, this Arg is also conserved in the ScPNPOx and MtPNPOx sequences and structural models (**Figure 4 and Figure 6**). Since allosteric regulation of PNPOx relies upon biomolecular conformations with their corresponding dynamic transitions, such insertion introduces steric obstacles impeding HsPNPOx to conserve exactly the same PLP allosteric site than EcPNPOx. In addition, the absence of the Arg23-Arg24 motif also indicates that allosteric sites in ScPNPOx and MtPNPOx might not be similarly conserved regarding EcPNPOx.

Some HsPNPOx structures showed a phosphate bound close to the PLP allosteric site in EcPNPOx, particularly surrounded by residues His248 and Arg249 sited in the strand C-terminal β-hairpin and nearly at the edge of the inter-subunit contact interface, and this site was at certain point proposed as potentially allocating the allosteric site. Such site would not be conserved in ScPNPOx or MtPNPOx, because their sequences are considerably shorter in this region. Nonetheless, the careful observation of these structures reveals for all of them other conserved patches of Arg residues that might form the cages to allocate PLP at the contact interface between both monomers in the homodimer. In HsPNPOx such patch might be made by the highly conserved Arg258 of one protomer together with Arg181 and Arg185 sited in the other protomer in one of the helices that undergo disorder upon PLP binding at the allosteric site in EcPNPOx (**Figure 6**). Noticeably, molecular dynamics simulations in HsPNPOx identified the 181–195 α6 helix and the 195–198 β-turn following it at the interdomain cap that folds out of the PNPOx and PNP_phzG_C domains of each protomer as the most flexible region of the protein [24]. Arg181 at the N-terminus of the longest helix is conserved in ScPNPOx and MtPNPOx (respectively as Arg160 and Arg162), but not Arg185. Nonetheless, in these two structures the respective Arg202 and Arg204 residues, sited in the first protomer in a long loop that protrudes inside the other protomer surface, are ready to close the cage (**Figure 6(b)**). Nonetheless, more recent docking, mutational and mechanistic studies indicate that in HsPNPOx both the C-terminal β-hairpin and the N-terminus of a same protomer will generate a cleft for the binding of allosteric PLP, which will be stabilized by His248 at the loop and the highly conserved Arg258 at the end of the second strand of the C-terminal β-hairpin, together with the side chains of Phe48 and Glu50 at the flexible N-terminus (see Figure 1 in [34]). Here, it is worth noticing the diversity of conformations among the five available HsPNPOx structures at the first residues detected at the N-terminus (residues 46-52), which suggests a conformational in such structural element when PLP binds at the allosteric site (see Figure 6 in [34]).

Preprints.org (www.preprints.org) | NOT PEER-REVIEWED | Posted: 19 February 2024 doi:10.20944/preprints202402.1002.v1

No His residue might replace for His248 in ScPNPOx and MtPNPOx, since, as in EcPNPOx, their short loops lack such residue. However, these two proteins show at their flexible N-terminus Phe and Glu/Asp residues that might make contribute to allosteric PLP binding as suggested in for HsPNPOx (**Figure 6(b)**). Therefore, despite in all evaluated PNPOxs the N-terminal and C-terminal of a same protomer appear as the main contributors to allosteric PLP binding, it is clear that the different length in the loop connecting the C-terminal β-hairpin will induce species-specific features. In agreement, and despite both HsPNPOx and EcPNPOx exhibiting PLP allosteric inhibition, the coupling between the allosteric and active sites appears notably weaker in HsPNPOx. In addition, while PLP does not bind at the active site of native EcPNPOx, HsPNPOx has demonstrated the capability to form a complex with two PLP molecules per protomer [18,21,23,27]. Such differences have been related to the binding of PLP at the allosteric site of EcPNPOx taking place with considerably higher affinity, and might be behind the differing kinetic inhibition models that describe this enzyme in different species.

Structural analyses also find MtPNPOx as the most divergent available experimental model. Noticeably, its crystal structure was reported in the absence of the FMN cofactor as well as any other ligand. Moreover, it lacks the arginine residue conserved as Arg88 in EcPNPOx, Arg166 in HsPNPOx, and Arg95 in ScPNPOx. Nonetheless, despite the conservation of such Arg and Glu189 in all these species at the FMN binding site, the Arg88-Glu189 salt-bridge present in EcPNPOx is not observed neither in HsPNPOx nor in ScPNPOx. Finally, it is also worth to note that the Cys residues at the monomers interface in HsPNPOx are absent in the other structures. All these features can therefore contribute to the intricate and reciprocal influence between PNP and PLP governing PNPOx activity in a species specific manner.

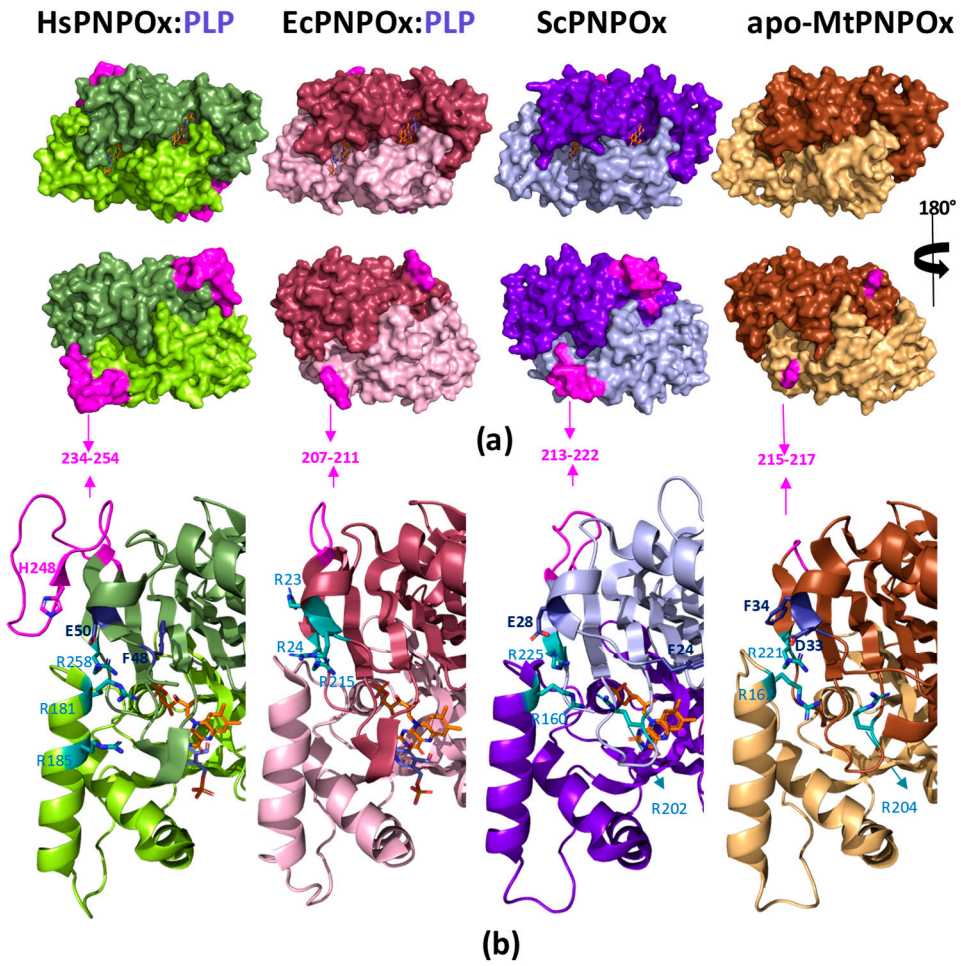

Figure 6. Species-specific structural features in PNPOx enzymes. (a) Surface representation of the crystallographic structure of the WT homodimers: from left to right HsPNPOx in complex with PLP

 doi:10.20944/preprints202402.1002.v1

at the active site (1NRG), EcPNPOx in complex with PLP at the active site (PDB 1G76), ScPNPOx (1CI0) and MtPNPOx (2A2J). **(b)** Detail of differential structural features. Arg residues that might form Arg cages at close positions to that determined in EcPNPOx as the allosteric PLP binding site are highlighted in CPK coloured sticks with carbons in deep teal. In HsPNPOx, in addition to Arg258, His248 (in CPK magenta sticks) at the loop connecting the C-terminal β–hairpin and F48 and E50 (in CPK dark blue stics) at the N-terminus have been proposed to replace the Arg cage in allosteric PLP binding. Potential equivalent residues in ScPNPOx and MtPNPOx structures are similarly highlighted. In all panels the loop connecting the C-terminal β–hairpin is highlighted in magenta, and each homodimer is shown in a different colour. FMN and PLP at active site, when present in structural models, are respectively shown in CPK sticks respectively coloured in orange and violet. Figure produced using PyMOL [35].

6. PNPOx and cofactor channelling

PLP-client enzymes first undergo biosynthesis in the apo-form, subsequently transitioning into the catalytically active holo-PLP enzymes through the covalent binding of PLP to an active site lysine to form an aldimine [21]. This process is noteworthy due to the reactivity of PLP, which can potentially form aldimines with free amino groups on non-PLP proteins and as a consequence disrupt their function [9]. To mitigate this toxicity, the cell maintains a low concentration of free PLP through its dephosphorylation as well as by PLP feedback inhibition of PNPOx and PLK [27,51-53]. However, it is noteworthy how maintaining such a low concentration of free cellular PLP allows activation of the large number of competing apo-PLP-dependent enzymes. A proposed protective mechanism would involve channelling of the newly formed PLP by PNPOx exclusively to its client apo-PLP-dependent enzymes, offering additional advantages such as reduced transit time, mitigating loss through diffusion and avoidance of competing metabolic pathways [51,54]. This hypothesis is supported by various biophysical and biochemical studies reporting complex formation of PNPOx with different apo-PLP-client enzymes [55-57]. Likely due to their transient nature, experimental structures for such complexes have not been reported so far. As an alternative, computational approaches have served to simulate how PNPOx recognizes and interacts with its potential partners. Such an approach, in combination with experimental biochemical evaluations, were used to examine how HsPNPOx and PLP-dependent dopa decarboxylase (HsDDC) might recognize and interact with each other. The results suggested contact between the allosteric PLP site on HsPNPOx and the PLP active site of the receptor as well as transient “loop-mediated” interactions between the two proteins, while demonstrating PNPOx's ability to both bind and transfer PLP (despite its tight binding) to apo-DDC [19].

Interestingly, the channelling approach in PNPOx may serve not only as a means to transfer its PLP product but also to integrate its own FMN cofactor, leading to the formation of the holo PNPOx state. Similarly to PLP, the FMN cofactor plays a crucial role in assisting the function of numerous flavoproteins and flavoenzymes within the cell (around 25% of flavoproteins use FMN in *Homo sapiens*), while maintaining its free concentration at a low level. FMN synthesis is catalysed by riboflavin kinase (RFK), and the transient interaction between RFK and PNPOx has been confirmed in the case of *H. sapiens* enzymes [24,58]. Furthermore, these studies have demonstrated the transfer of tightly bound FMN from HsRFK to apo-HsPNPOx, as well as mutual influence between the two proteins in catalysis and ligand binding steps. Plausible binding modes of HsRFK binding to HsPNPOx have been simulated, envisioning coupling between their respective FMN binding cavities. Various complex arrangements are envisaged to result from diverse ligation and conformational states expected for HsRFK during catalysis, particularly influenced by changes in conformation of the loops forming the FMN binding site and its exit channel [58]. Importantly, predictions suggest that loops in HsPNPOx also contribute to protein-protein fitting, hinting again at transient "loop-mediated" interactions whose reorganization might mediate cofactor transfer [24]. Altogether, an intricate thermodynamic landscape governing binding and transference, and highly sensitive to particular HsRFK and HsPNPOx ligation states, was proposed to regulate coupling and overall channelling processes between these two proteins [24]. Residues predicted to be involved in

this interaction in HsPNPOx were located in α1 (Phe66 and Glu67) and α4-tun (Glu152-Glu153, Glu155, Tyr157-Phe158 and Arg161-Pro162), and to a lesser extent in the β3-β4-hairpin (Phe102 and Arg108). Noticeably, some of these residues are conserved in EcPNPOx, ScPNPOx and MtPNPOx, especially those in α1 (Phe35 and Glu36 in EcPNPOx and Phe43 and Glu45 in ScPNPOx) and α4-turn (Glu125, Tyr129-Phe130 and Arg133-Pro134 in EcPNPOx; Glu131, Glu134, Tyr136-Phe137 and Arg140-Pro141 in ScPNPOx; and Glu133-Glu134, Tyr138, Arg142-Pro143 in MtPNPOx).

7. Conclusions

The so far available functional and structural information across different organisms provides interesting insights into the mechanism governing PNPOx activity. Moreover, it indicates that while there may be shared characteristics, PNPOx will exhibit some unique species-specific features tailored to regulate PNPOx activity. Such diversity in PNPOx regulation highlights the adaptability of its intricate mechanisms to meet the distinct needs of individual organisms, and might be relevant in the future development of therapies having it as a target.

Author Contributions: Conceptualization, M.M.; software, M.M. and M.R.; formal analysis, M.M., M.R. and N.N.; investigation, M.M., M.R. and N.N.; data curation, M.M.; writing—original draft preparation, M.M.; writing—review and editing, M.M., M.R. and N.N.; visualization, M.M.; supervision, M.M.; project administration, M.M.; funding acquisition, M.M. All authors have read and agreed to the published version of the manuscript.

Funding: This research was funded by MCIN/AEI/10.13039/501100011033/ERDF, grant number MCIN/AEI/PID2022-136369NB-I00 and Gobierno de Aragon, Grant number E35-23R. "The APC was funded by CIN/AEI/PID2022-136369NB-I00.

Institutional Review Board Statement: Not applicable.

Informed Consent Statement: Not applicable.

Data Availability Statement: The data presented in this study derived from public databases, namely PDB [https://www.rcsb.org/] and public bibliographic databases such as PubMed [https://pubmed.ncbi.nlm.nih.gov/].

Conflicts of Interest: The authors declare no conflicts of interest.

References

1. Wilson, M.P.; Plecko, B.; Mills, P.B.; Clayton, P.T. Disorders affecting vitamin B metabolism. *J Inherit Metab Dis* **2019**, *42*, 629-646, doi:10.1002/jimd.12060.
2. Parra, M.; Stahl, S.; Hellmann, H. Vitamin B_6 and Its Role in Cell Metabolism and Physiology. *Cells* **2018**, *7*, doi:10.3390/cells7070084.
3. Guerriero, R.M.; Patel, A.A.; Walsh, B.; Baumer, F.M.; Shah, A.S.; Peters, J.M.; Rodan, L.H.; Agrawal, P.B.; Pearl, P.L.; Takeoka, M. Systemic Manifestations in Pyridox(am)ine 5'-Phosphate Oxidase Deficiency. *Pediatr Neurol* **2017**, *76*, 47-53, doi:10.1016/j.pediatrneurol.2017.05.024.
4. Percudani, R.; Peracchi, A. A genomic overview of pyridoxal-phosphate-dependent enzymes. *EMBO Rep* **2003**, *4*, 850-854, doi:10.1038/sj.embor.embor914.
5. Percudani, R.; Peracchi, A. The B6 database: a tool for the description and classification of vitamin B6-dependent enzymatic activities and of the corresponding protein families. *BMC Bioinformatics* **2009**, *10*, 273, doi:10.1186/1471-2105-10-273.
6. Gachon, F.; Fonjallaz, P.; Damiola, F.; Gos, P.; Kodama, T.; Zakany, J.; Duboule, D.; Petit, B.; Tafti, M.; Schibler, U. The loss of circadian PAR bZip transcription factors results in epilepsy. *Genes Dev* **2004**, *18*, 1397-1412, doi:10.1101/gad.301404.
7. Laber, B.; Maurer, W.; Scharf, S.; Stepusin, K.; Schmidt, F.S. Vitamin B6 biosynthesis: formation of pyridoxine 5'-phosphate from 4-(phosphohydroxy)-L-threonine and 1-deoxy-D-xylulose-5-phosphate by PdxA and PdxJ protein. *FEBS Lett* **1999**, *449*, 45-48, doi:10.1016/s0014-5793(99)00393-2.
8. Tambasco-Studart, M.; Titiz, O.; Raschle, T.; Forster, G.; Amrhein, N.; Fitzpatrick, T.B. Vitamin B6 biosynthesis in higher plants. *Proc Natl Acad Sci U S A* **2005**, *102*, 13687-13692, doi:10.1073/pnas.0506228102.
9. di Salvo, M.L.; Safo, M.K.; Contestabile, R. Biomedical aspects of pyridoxal 5'-phosphate availability. *Front Biosci (Elite Ed)* **2012**, *4*, 897-913, doi:10.2741/E428.
10. Said, H.M. Intestinal absorption of water-soluble vitamins in health and disease. *Biochem J* **2011**, *437*, 357-372, doi:10.1042/BJ20110326.

11. Denise, R.; Babor, J.; Gerlt, J.A.; de Crécy-Lagard, V. Pyridoxal 5'-phosphate synthesis and salvage in Bacteria and Archaea: predicting pathway variant distributions and holes. *Microb Genom* **2023**, *9*, doi:10.1099/mgen.0.000926.
12. Gregory, J.F. Nutritional Properties and significance of vitamin glycosides. *Annu Rev Nutr* **1998**, *18*, 277-296, doi:10.1146/annurev.nutr.18.1.277.
13. Said, Z.M.; Subramanian, V.S.; Vaziri, N.D.; Said, H.M. Pyridoxine uptake by colonocytes: a specific and regulated carrier-mediated process. *Am J Physiol Cell Physiol* **2008**, *294*, C1192-1197, doi:10.1152/ajpcell.00015.2008.
14. Suvorova, I.A.; Rodionov, D.A. Comparative genomics of pyridoxal 5'-phosphate-dependent transcription factor regulons in. *Microb Genom* **2016**, *2*, e000047, doi:10.1099/mgen.0.000047.
15. Said, H.M.; Ortiz, A.; Ma, T.Y. A carrier-mediated mechanism for pyridoxine uptake by human intestinal epithelial Caco-2 cells: regulation by a PKA-mediated pathway. *Am J Physiol Cell Physiol* **2003**, *285*, C1219-1225, doi:10.1152/ajpcell.00204.2003.
16. Miyake, K.; Yasujima, T.; Takahashi, S.; Yamashiro, T.; Yuasa, H. Identification of the amino acid residues involved in the species-dependent differences in the pyridoxine transport function of SLC19A3. *J Biol Chem* **2022**, *298*, 102161, doi:10.1016/j.jbc.2022.102161.
17. Stolz, J.; Vielreicher, M. Tpn1p, the plasma membrane vitamin B6 transporter of Saccharomyces cerevisiae. *J Biol Chem* **2003**, *278*, 18990-18996, doi:10.1074/jbc.M300949200.
18. Barile, A.; Battista, T.; Fiorillo, A.; di Salvo, M.L.; Malatesta, F.; Tramonti, A.; Ilari, A.; Contestabile, R. Identification and characterization of the pyridoxal 5'-phosphate allosteric site in Escherichia coli pyridoxine 5'-phosphate oxidase. *J Biol Chem* **2021**, *296*, 100795, doi:10.1016/j.jbc.2021.100795.
19. Al Mughram, M.H.; Ghatge, M.S.; Kellogg, G.E.; Safo, M.K. Elucidating the Interaction between Pyridoxine 5'-Phosphate Oxidase and Dopa Decarboxylase: Activation of B6-Dependent Enzyme. *Int J Mol Sci* **2022**, *24*, doi:10.3390/ijms24010642.
20. Kang, J.H.; Hong, M.L.; Kim, D.W.; Park, J.; Kang, T.C.; Won, M.H.; Baek, N.I.; Moon, B.J.; Choi, S.Y.; Kwon, O.S. Genomic organization, tissue distribution and deletion mutation of human pyridoxine 5'-phosphate oxidase. *Eur J Biochem* **2004**, *271*, 2452-2461, doi:10.1111/j.1432-1033.2004.04175.x.
21. Musayev, F.N.; Di Salvo, M.L.; Ko, T.P.; Schirch, V.; Safo, M.K. Structure and properties of recombinant human pyridoxine 5'-phosphate oxidase. *Protein Sci* **2003**, *12*, 1455-1463, doi:10.1110/ps.0356203.
22. Musayev, F.N.; Di Salvo, M.L.; Saavedra, M.A.; Contestabile, R.; Ghatge, M.S.; Haynes, A.; Schirch, V.; Safo, M.K. Molecular basis of reduced pyridoxine 5'-phosphate oxidase catalytic activity in neonatal epileptic encephalopathy disorder. *J Biol Chem* **2009**, *284*, 30949-30956, doi:10.1074/jbc.M109.038372.
23. Barile, A.; Nogués, I.; di Salvo, M.L.; Bunik, V.; Contestabile, R.; Tramonti, A. Molecular characterization of pyridoxine 5'-phosphate oxidase and its pathogenic forms associated with neonatal epileptic encephalopathy. *Sci Rep* **2020**, *10*, 13621, doi:10.1038/s41598-020-70598-7.
24. Rivero, M.; Boneta, S.; Novo, N.; Velázquez-Campoy, A.; Polo, V.; Medina, M. Riboflavin kinase and pyridoxine 5'-phosphate oxidase complex formation envisages transient interactions for FMN cofactor delivery. *Front Mol Biosci* **2023**, *10*, 1167348, doi:10.3389/fmolb.2023.1167348.
25. Di Salvo, M.; Yang, E.; Zhao, G.; Winkler, M.E.; Schirch, V. Expression, purification, and characterization of recombinant Escherichia coli pyridoxine 5'-phosphate oxidase. *Protein Expr Purif* **1998**, *13*, 349-356, doi:10.1006/prep.1998.0904.
26. Zhao, G.; Winkler, M.E. Kinetic limitation and cellular amount of pyridoxine (pyridoxamine) 5'-phosphate oxidase of Escherichia coli K-12. *J Bacteriol* **1995**, *177*, 883-891, doi:10.1128/jb.177.4.883-891.1995.
27. Barile, A.; Tramonti, A.; di Salvo, M.L.; Nogués, I.; Nardella, C.; Malatesta, F.; Contestabile, R. Allosteric feedback inhibition of pyridoxine 5'-phosphate oxidase from. *J Biol Chem* **2019**, *294*, 15593-15603, doi:10.1074/jbc.RA119.009697.
28. Kim, Y.T.; Churchich, J.E. Sequence of the cysteinyl-containing peptides of 4-aminobutyrate aminotransferase. Identification of sulfhydryl residues involved in intersubunit linkage. *Eur J Biochem* **1989**, *181*, 397-401, doi:10.1111/j.1432-1033.1989.tb14738.x.
29. Choi, S.Y.; Churchich, J.E.; Zaiden, E.; Kwok, F. Brain pyridoxine-5-phosphate oxidase. Modulation of its catalytic activity by reaction with pyridoxal 5-phosphate and analogs. *J Biol Chem* **1987**, *262*, 12013-12017.
30. Kazarinoff, M.N.; McCormick, D.B. Rabbit liver pyridoxamine (pyridoxine) 5'-phosphate oxidase. Purification and properties. *J Biol Chem* **1975**, *250*, 3436-3442.
31. Choi, J.D.; Bowers-Komro, M.; Davis, M.D.; Edmondson, D.E.; McCormick, D.B. Kinetic properties of pyridoxamine (pyridoxine)-5'-phosphate oxidase from rabbit liver. *J Biol Chem* **1983**, *258*, 840-845.
32. Churchich, J.E. Brain pyridoxine-5-phosphate oxidase. A dimeric enzyme containing one FMN site. *Eur J Biochem* **1984**, *138*, 327-332, doi:10.1111/j.1432-1033.1984.tb07918.x.
33. Safo, M.K.; Musayev, F.N.; Schirch, V. Structure of Escherichia coli pyridoxine 5'-phosphate oxidase in a tetragonal crystal form: insights into the mechanistic pathway of the enzyme. *Acta Crystallogr D Biol Crystallogr* **2005**, *61*, 599-604, doi:10.1107/S0907444905005512.

34. Barile, A.; Graziani, C.; Antonelli, L.; Parroni, A.; Fiorillo, A.; di Salvo, M.L.; Ilari, A.; Giorgi, A.; Rosignoli, S.; Paiardini, A.; et al. Identification of the pyridoxal 5'-phosphate allosteric site in human pyridox(am)ine 5'-phosphate oxidase. *Protein Sci* **2024**, *33*, e4900, doi:10.1002/pro.4900.
35. Delano, W.L. PyMOL: an open-source molecular graphics tool. *CCP4 Newsletter On Protein Crystallography* **2002**, *40*, 82-92.
36. Ghatge, M.S.; Al Mughram, M.; Omar, A.M.; Safo, M.K. Inborn errors in the vitamin B6 salvage enzymes associated with neonatal epileptic encephalopathy and other pathologies. *Biochimie* **2021**, *183*, 18-29, doi:10.1016/j.biochi.2020.12.025.
37. Barile, A.; Mills, P.; di Salvo, M.L.; Graziani, C.; Bunik, V.; Clayton, P.; Contestabile, R.; Tramonti, A. Characterization of Novel Pathogenic Variants Causing Pyridox(am)ine 5'-Phosphate Oxidase-Dependent Epilepsy. *Int J Mol Sci* **2021**, *22*, doi:10.3390/ijms222112013.
38. Alghamdi, M.; Bashiri, F.A.; Abdelhakim, M.; Adly, N.; Jamjoom, D.Z.; Sumaily, K.M.; Alghanem, B.; Arold, S.T. Phenotypic and molecular spectrum of pyridoxamine-5'-phosphate oxidase deficiency: A scoping review of 87 cases of pyridoxamine-5'-phosphate oxidase deficiency. *Clin Genet* **2021**, *99*, 99-110, doi:10.1111/cge.13843.
39. Guerin, A.; Aziz, A.S.; Mutch, C.; Lewis, J.; Go, C.Y.; Mercimek-Mahmutoglu, S. Pyridox(am)ine-5-Phosphate Oxidase Deficiency Treatable Cause of Neonatal Epileptic Encephalopathy With Burst Suppression: Case Report and Review of the Literature. *J Child Neurol* **2015**, *30*, 1218-1225, doi:10.1177/0883073814550829.
40. Mills, P.B.; Camuzeaux, S.S.; Footitt, E.J.; Mills, K.A.; Gissen, P.; Fisher, L.; Das, K.B.; Varadkar, S.M.; Zuberi, S.; McWilliam, R.; et al. Epilepsy due to PNPO mutations: genotype, environment and treatment affect presentation and outcome. *Brain* **2014**, *137*, 1350-1360, doi:10.1093/brain/awu051.
41. Khayat, M.; Korman, S.H.; Frankel, P.; Weintraub, Z.; Hershckowitz, S.; Sheffer, V.F.; Elisha, M.B.; Wevers, R.A.; Falik-Zaccai, T.C. PNPO deficiency: an under diagnosed inborn error of pyridoxine metabolism. *Mol Genet Metab* **2008**, *94*, 431-434, doi:10.1016/j.ymgme.2008.04.008.
42. Plecko, B.; Paul, K.; Mills, P.; Clayton, P.; Paschke, E.; Maier, O.; Hasselmann, O.; Schmiedel, G.; Kanz, S.; Connolly, M.; et al. Pyridoxine responsiveness in novel mutations of the PNPO gene. *Neurology* **2014**, *82*, 1425-1433, doi:10.1212/WNL.0000000000000344.
43. Jaeger, B.; Abeling, N.G.; Salomons, G.S.; Struys, E.A.; Simas-Mendes, M.; Geukers, V.G.; Poll-The, B.T. Pyridoxine responsive epilepsy caused by a novel homozygous PNPO mutation. *Mol Genet Metab Rep* **2016**, *6*, 60-63, doi:10.1016/j.ymgmr.2016.01.004.
44. Hoffmann, G.F.; Schmitt, B.; Windfuhr, M.; Wagner, N.; Strehl, H.; Bagci, S.; Franz, A.R.; Mills, P.B.; Clayton, P.T.; Baumgartner, M.R.; et al. Pyridoxal 5'-phosphate may be curative in early-onset epileptic encephalopathy. *J Inherit Metab Dis* **2007**, *30*, 96-99, doi:10.1007/s10545-006-0508-4.
45. Ware, T.L.; Earl, J.; Salomons, G.S.; Struys, E.A.; Peters, H.L.; Howell, K.B.; Pitt, J.J.; Freeman, J.L. Typical and atypical phenotypes of PNPO deficiency with elevated CSF and plasma pyridoxamine on treatment. *Dev Med Child Neurol* **2014**, *56*, 498-502, doi:10.1111/dmcn.12346.
46. Mills, P.B.; Surtees, R.A.; Champion, M.P.; Beesley, C.E.; Dalton, N.; Scambler, P.J.; Heales, S.J.; Briddon, A.; Scheimberg, I.; Hoffmann, G.F.; et al. Neonatal epileptic encephalopathy caused by mutations in the PNPO gene encoding pyridox(am)ine 5'-phosphate oxidase. *Hum Mol Genet* **2005**, *14*, 1077-1086, doi:10.1093/hmg/ddi120.
47. di Salvo, M.L.; Mastrangelo, M.; Nogués, I.; Tolve, M.; Paiardini, A.; Carducci, C.; Mei, D.; Montomoli, M.; Tramonti, A.; Guerrini, R.; et al. Biochemical data from the characterization of a new pathogenic mutation of human pyridoxine-5'-phosphate oxidase (PNPO). *Data Brief* **2017**, *15*, 868-875, doi:10.1016/j.dib.2017.10.032.
48. di Salvo, M.L.; Mastrangelo, M.; Nogués, I.; Tolve, M.; Paiardini, A.; Carducci, C.; Mei, D.; Montomoli, M.; Tramonti, A.; Guerrini, R.; et al. Pyridoxine-5'-phosphate oxidase (Pnpo) deficiency: Clinical and biochemical alterations associated with the C.347g>A (P.·Arg116gln) mutation. *Mol Genet Metab* **2017**, *122*, 135-142, doi:10.1016/j.ymgme.2017.08.003.
49. Yang, E.S.; Schirch, V. Tight binding of pyridoxal 5'-phosphate to recombinant Escherichia coli pyridoxine 5'-phosphate oxidase. *Arch Biochem Biophys* **2000**, *377*, 109-114, doi:10.1006/abbi.2000.1737.
50. di Salvo, M.L.; Ko, T.P.; Musayev, F.N.; Raboni, S.; Schirch, V.; Safo, M.K. Active site structure and stereospecificity of Escherichia coli pyridoxine-5'-phosphate oxidase. *J Mol Biol* **2002**, *315*, 385-397, doi:10.1006/jmbi.2001.5254.
51. di Salvo, M.L.; Contestabile, R.; Safo, M.K. Vitamin B(6) salvage enzymes: mechanism, structure and regulation. *Biochim Biophys Acta* **2011**, *1814*, 1597-1608, doi:10.1016/j.bbapap.2010.12.006.
52. Whittaker, J.W. Intracellular trafficking of the pyridoxal cofactor. Implications for health and metabolic disease. *Arch Biochem Biophys* **2016**, *592*, 20-26, doi:10.1016/j.abb.2015.11.031.
53. Ghatge, M.S.; Contestabile, R.; di Salvo, M.L.; Desai, J.V.; Gandhi, A.K.; Camara, C.M.; Florio, R.; González, I.N.; Parroni, A.; Schirch, V.; et al. Pyridoxal 5'-phosphate is a slow tight binding inhibitor of E. coli pyridoxal kinase. *PLoS One* **2012**, *7*, e41680, doi:10.1371/journal.pone.0041680.

 doi:10.20944/preprints202402.1002.v1

54. Miles, E.W.; Rhee, S.; Davies, D.R. The molecular basis of substrate channeling. *J Biol Chem* **1999**, *274*, 12193-12196, doi:10.1074/jbc.274.18.12193.
55. Ghatge, M.S.; Karve, S.S.; David, T.M.; Ahmed, M.H.; Musayev, F.N.; Cunningham, K.; Schirch, V.; Safo, M.K. Inactive mutants of human pyridoxine 5'-phosphate oxidase: a possible role for a noncatalytic pyridoxal 5'-phosphate tight binding site. *FEBS Open Bio* **2016**, *6*, 398-408, doi:10.1002/2211-5463.12042.
56. Kim, Y.T.; Kwok, F.; Churchich, J.E. Interactions of pyridoxal kinase and aspartate aminotransferase emission anisotropy and compartmentation studies. *J Biol Chem* **1988**, *263*, 13712-13717.
57. Cheung, P.Y.; Fong, C.C.; Ng, K.T.; Lam, W.C.; Leung, Y.C.; Tsang, C.W.; Yang, M.; Wong, M.S. Interaction between pyridoxal kinase and pyridoxal-5-phosphate-dependent enzymes. *J Biochem* **2003**, *134*, 731-738, doi:10.1093/jb/mvg201.
58. Anoz-Carbonell, E.; Rivero, M.; Polo, V.; Velázquez-Campoy, A.; Medina, M. Human riboflavin kinase: Species-specific traits in the biosynthesis of the FMN cofactor. *FASEB J* **2020**, *34*, 10871-10886, doi:10.1096/fj.202000566R.